Fig. S1. Targeting endogenous α-catenin to mitochondria does not affect α-catenin levels at cell-cell junctions. (A) β-Cat-ActA MDCK cells mixed with MDCK WT cells were fixed and stained for α-catenin (FITC). β-Cat-ActA MDCK cells express RFP, whereas WT MDCK cells do not. Images were acquired with AxioVision software (Zeiss) and a Zeiss Axiovert 200M inverted microscope equipped with a 63x oil objective. Displayed images are representative of three independent experiments. Scale bar, 20 μm. **(B)** The mean fluorescence intensity (MFI) of α-catenin at cell-cell contacts was quantified between two RFP expressing cells (E:E), an RFP-expressing and non-expressing cell (E:N), and two non-expressing cells (N:N) using ImageJ. The ends of the box and whisker plot represent the first and third quartiles, the horizontal line represents the median, and the whiskers represent the highest and lowest values within 1.5 times the interquartile range. Diamonds represent outliers. For each condition, $n > 30$ different cell-cell contacts.

Fig. S2. Force-dependent distributions of F-actin and vinculin at bead-cell junctions. (A) Original images of F-actin distributions in R2/7 Rescued cells bound with PLL beads. Imaging with a 40x objective reveals the overall cell monolayer, and the boxed regions (DIC channel) correspond to the cropped and zoomed-in images of individual beads, displayed in Figure 4B. Scale bars, 10 μm. **(B)** R2/7 Rescued, R2/7, and R2/7 ΔVBS cells bound with E-cadherin beads were fixed and stained for F-actin or vinculin before or after applying shear stress. Boxed regions in the DIC channel correspond to Figure 4C-H. Scale bars, 10 μm.

Fig. S3. Line-scan analyses of force-dependent distributions of α-catenin, F-actin, and vinculin at bead-cell junctions. (A) Representative line scans quantifying mean pixel intensity of GFP-α-catenin across bead-cell junctions before (-) or after (+) applying shear stress. Line scans were performed as described in *Materials and Methods*. R2/7 Rescued, R2/7, and R2/7 ΔVBS cells were bound with E-cadherin beads. **(B)** Representative line scans reveal F-actin distributions across bead-cell junctions in cells bound with E-cadherin beads, or PLL beads as noted. **(C)** Representative line scans reveal vinculin distributions across bead-cell junctions.

Fig. S4. Representative traction force maps that correspond to Fig. 7C. RMS traction forces exerted by R2/7, R2/7 ΔVBS, R2/7 Rescued, and DLD-1 cells on soft (1 kPa), semi-rigid (9 kPa), and rigid (34 kPa) hydrogels coated with E-cad-Fc. For each condition, maps are representative of $n \geq 10$ different cells.

A

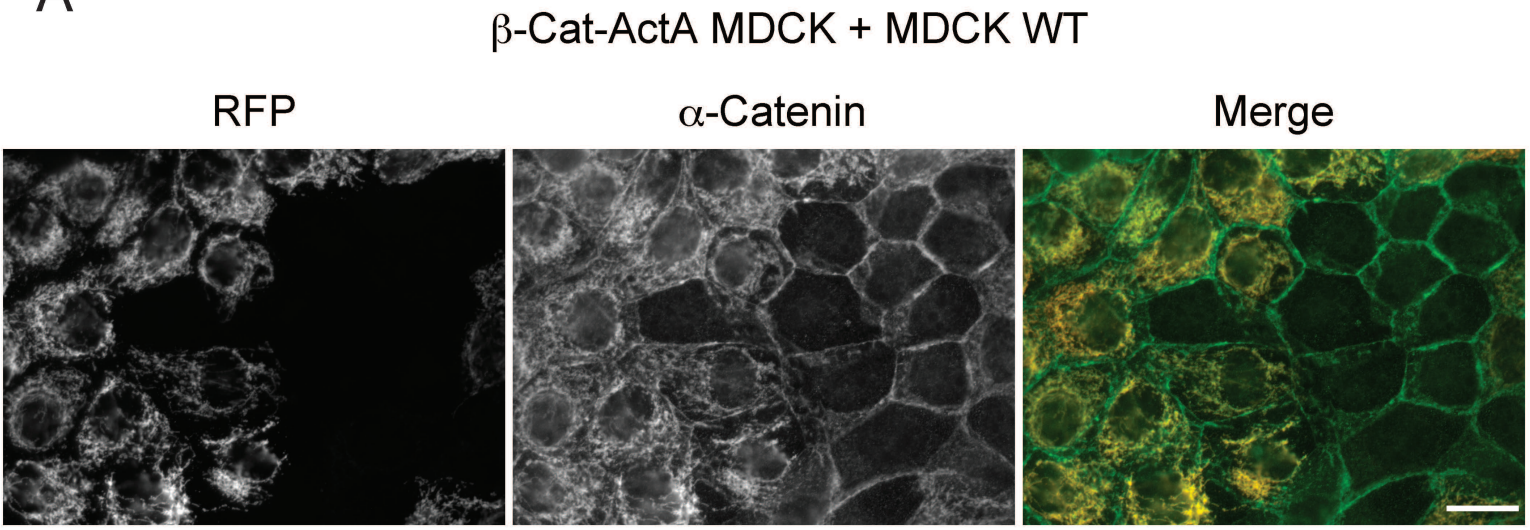

B

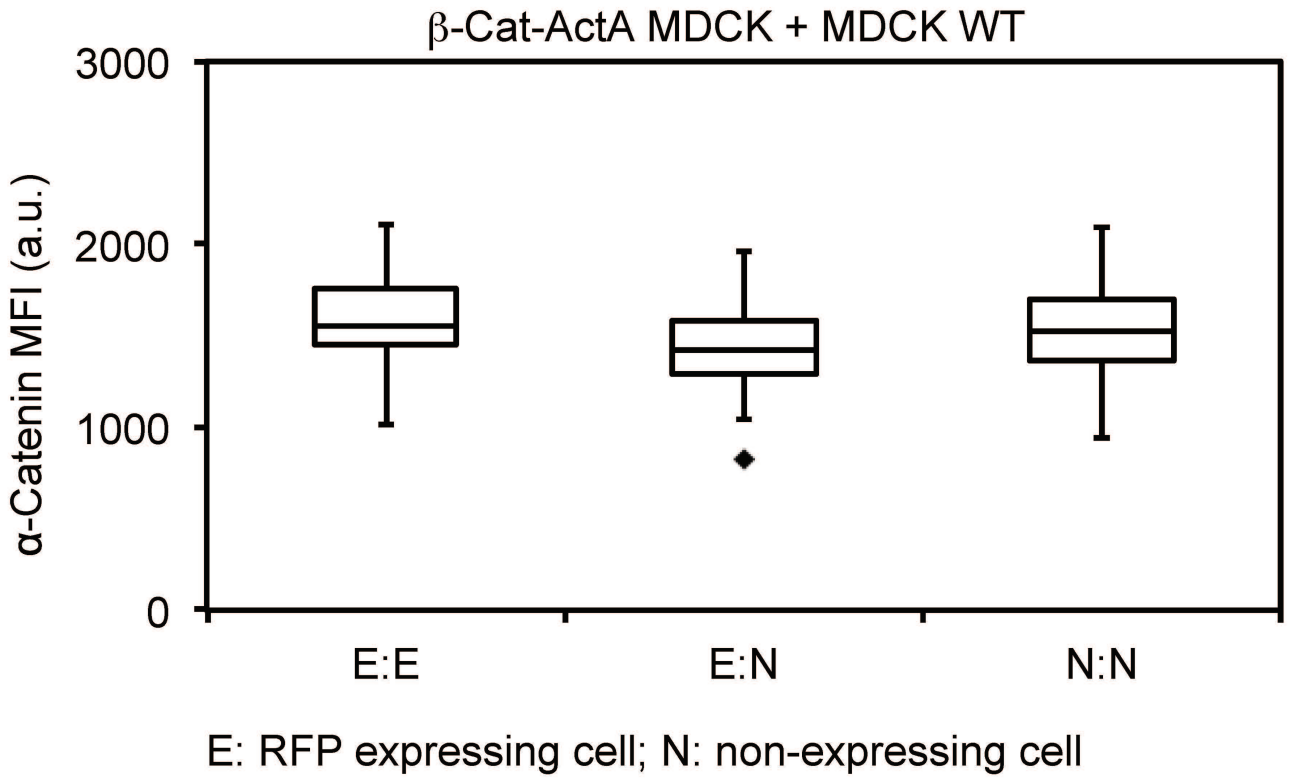

E: RFP expressing cell; N: non-expressing cell

Figure S1

A

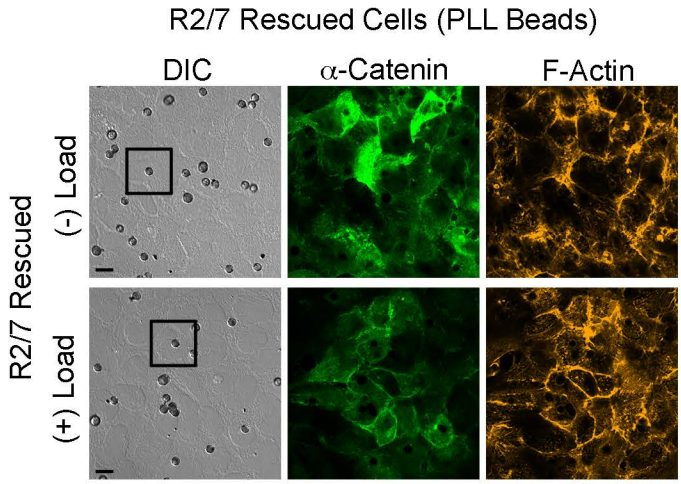
R2/7 Rescued Cells (PLL Beads)
DIC
α-Catenin
F-Actin
R2/7 Rescued
(-) Load
(+) Load

B

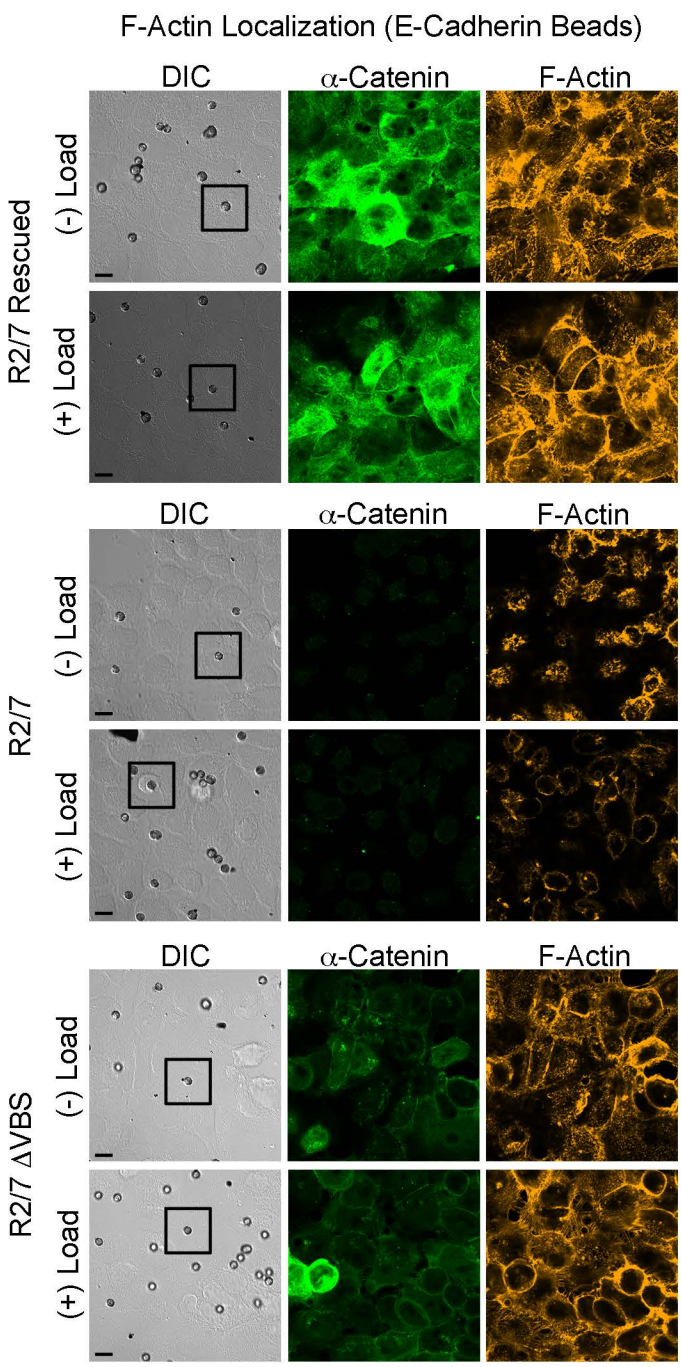
F-Actin Localization (E-Cadherin Beads)
DIC
α-Catenin
F-Actin
R2/7 Rescued
R2/7
R2/7 ΔVBS
(-) Load
(+) Load

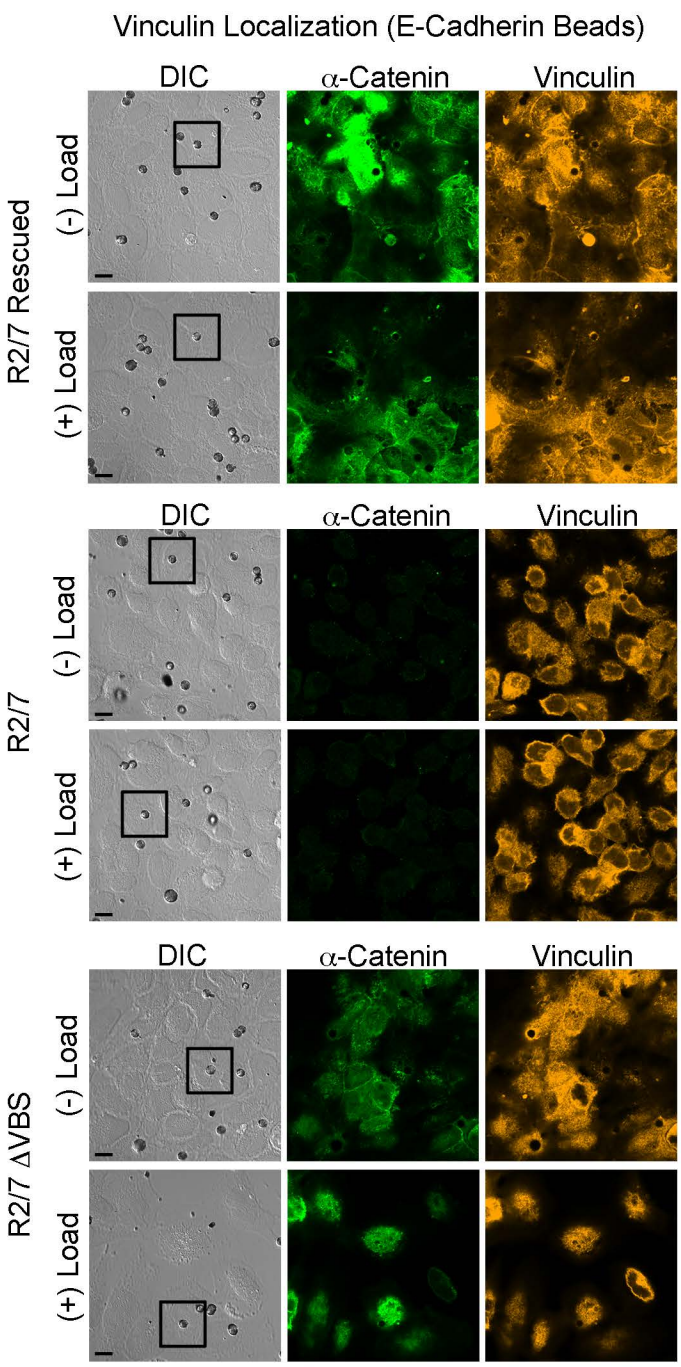
Vinculin Localization (E-Cadherin Beads)
DIC
α-Catenin
Vinculin
R2/7 Rescued
R2/7
R2/7 ΔVBS
(-) Load
(+) Load

A

α-Catenin

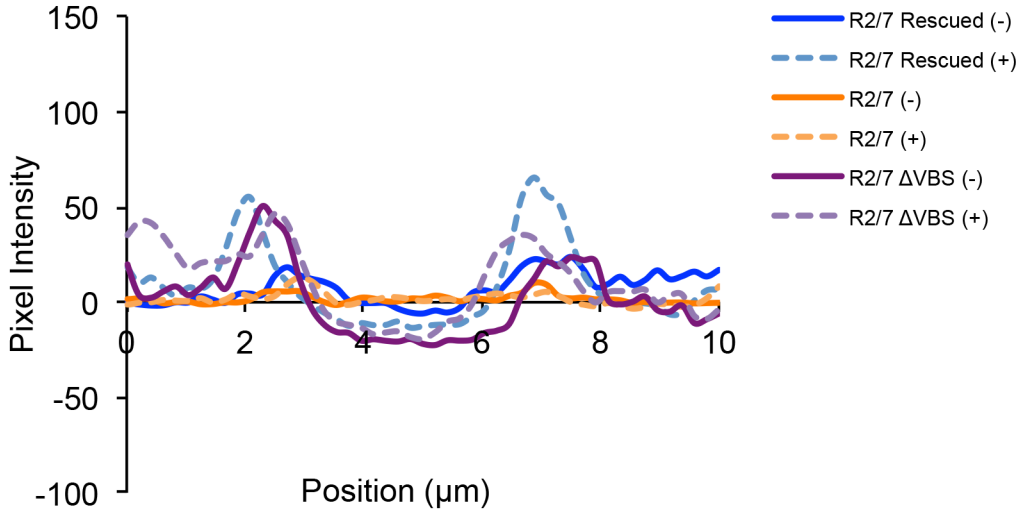

B

F-Actin

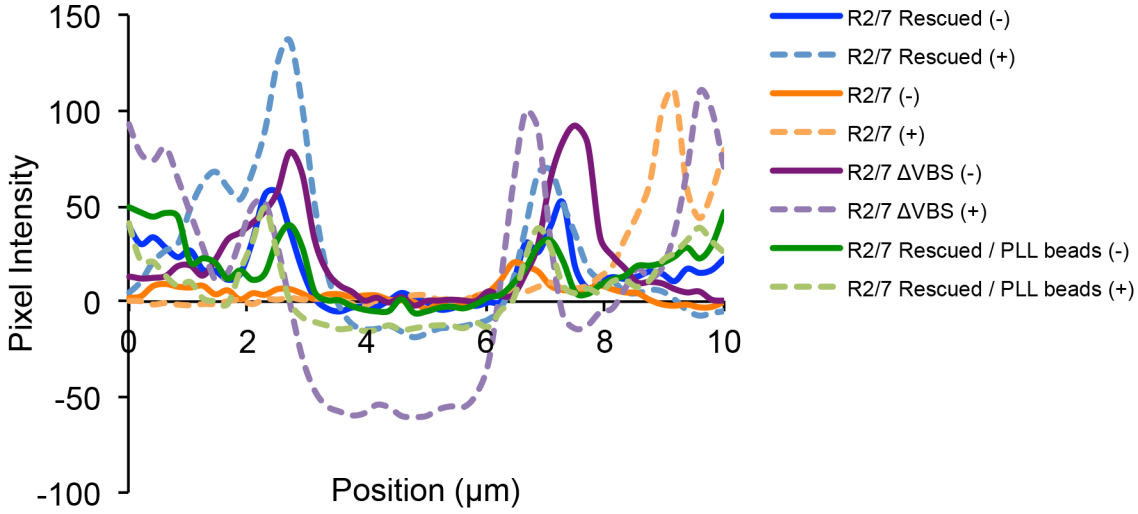

C

Vinculin

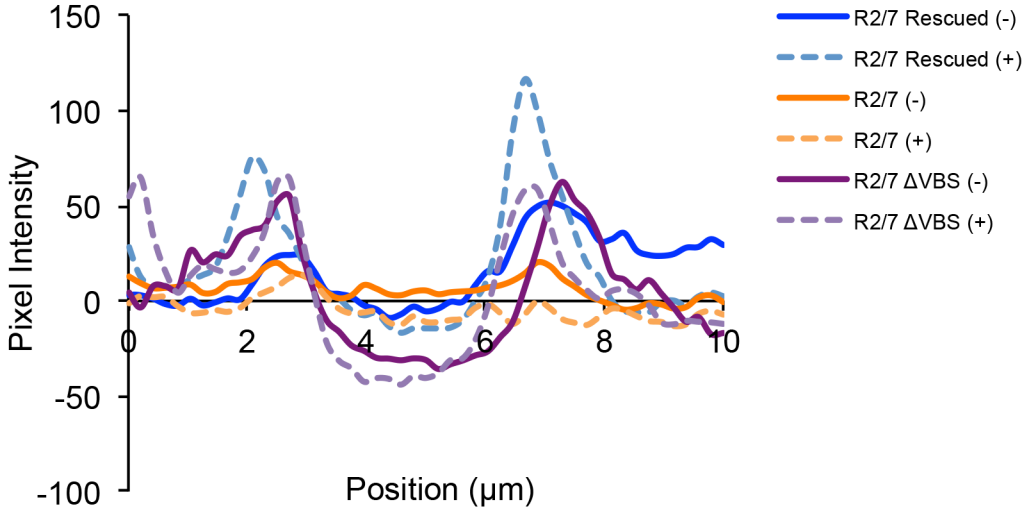

Figure S3

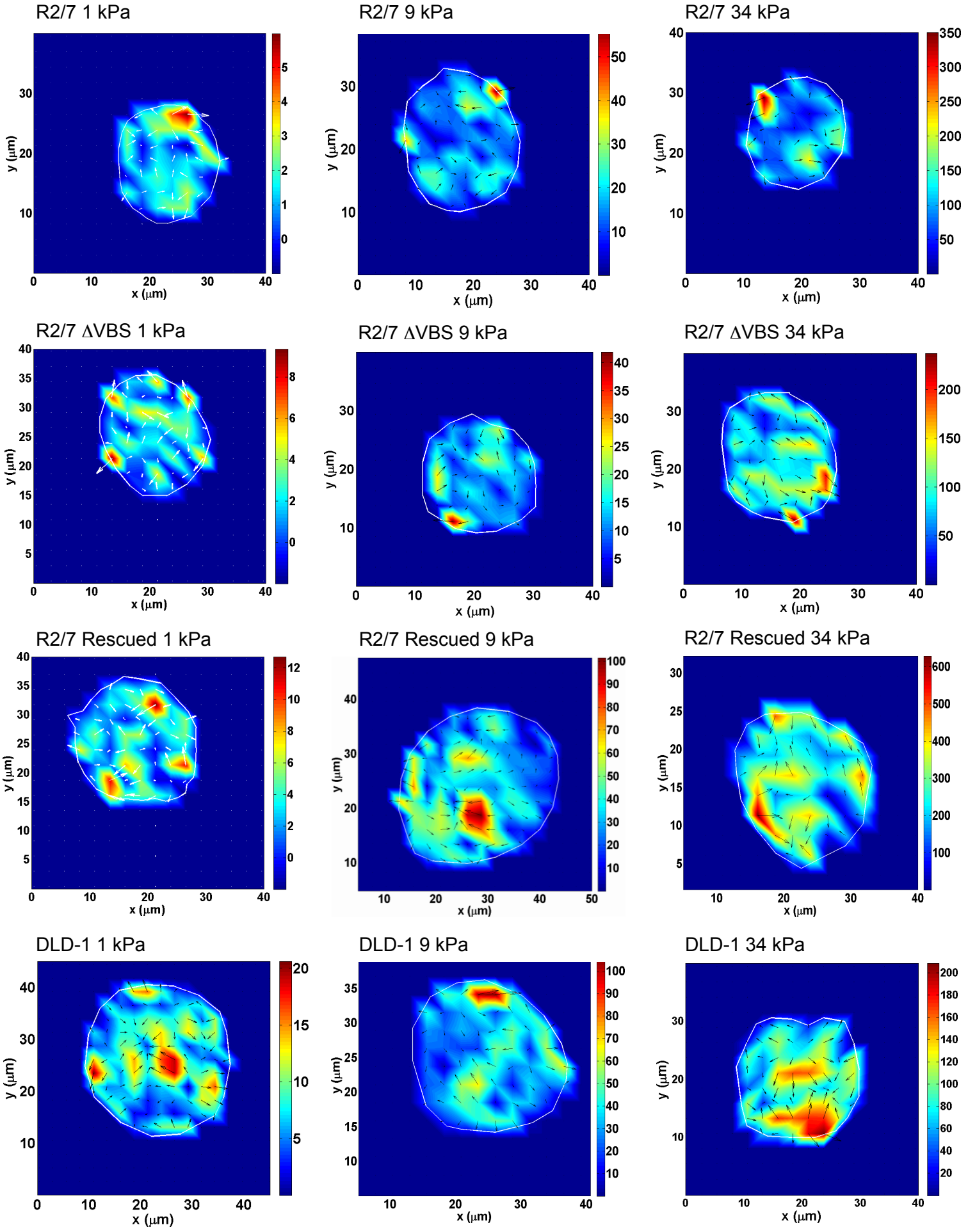
R2/7 1 kPa
R2/7 9 kPa
R2/7 34 kPa
R2/7 ΔVBS 1 kPa
R2/7 ΔVBS 9 kPa
R2/7 ΔVBS 34 kPa
R2/7 Rescued 1 kPa
R2/7 Rescued 9 kPa
R2/7 Rescued 34 kPa
DLD-1 1 kPa
DLD-1 9 kPa
DLD-1 34 kPa
x (μm)
y (μm)

Figure S4